THE ASTROPHYSICAL JOURNAL, 409:691–696, 1993 June 1

DISCONTINUITIES IN THE DYNAMIC SPECTRUM OF THE PULSAR 0823+26

ANDREW W. CLEGG,[1,2] RALPH L. FIEDLER,[1] AND JAMES M. CORDES[3]

Received 1992 September 11; accepted 1992 December 7

ABSTRACT

The 1400 MHz dynamic spectrum of the pulsar 0823+26 exhibits sharp discontinuities which are characterized by changes in the diffractive scintillation pattern over transition times of $\lesssim 2$ minutes. The discontinuities occur during periods in which the pulsar's broad-band (40 MHz) light curve is undergoing strong oscillations with periods of ~ 15 minutes. We believe these effects are due to coherent interference between multiple images created by strong refraction in the interstellar medium. In effect, we observe the discontinuities in the dynamic spectrum when the scintillation patterns of different images (each traveling different optical paths) alternately dominate the received intensity. The light curve oscillations are caused by coherent interference between the various images over bandwidths greater than the observing bandwidth. Based on the time scale for the oscillations at 1400 MHz, we derive a characteristic angular offset between images of approximately 0.5 mas. We cannot determine if the strong refraction is a consequence of the statistical nature of the medium along this line-of-sight, or whether a discrete refractor (i.e., an interstellar lens) is responsible. If the refractor is a discrete object, its dimension transverse to the line-of-sight is $\gtrsim 0.19f$ AU and its electron column density is $\gtrsim 1.2 \times 10^{-4} f$ cm^{-3} pc, where f is the fractional distance of the refractor along the line-of-sight to the pulsar. Its electron number density is $\sim 123/\eta$ cm^{-3}, where η is the elongation of the refractor along the line-of-sight relative to its transverse dimension. The pulsar 0823+26 is a promising candidate for interstellar interferometry since it apparently undergoes extended periods of multiple imaging.

Subject headings: ISM: general — pulsars: individual (PSR 0823+26)

1. INTRODUCTION

A variety of refraction effects in pulsar dynamic spectra have been previously reported (Rickett 1990). Some of these effects are consistent with strong refraction in which ray crossing occurs and multiple images of the pulsar are formed. The coherent interference between multiple images, visible as fringes in the time/frequency domain, has been exploited to resolve or constrain spatial structure in pulsar magnetospheres on angular scales of $\lesssim 1$ μas (Wolszczan & Cordes 1987).

In order to study strong refraction effects in pulsar dynamic spectra, we monitored a set of pulsars daily or every other day over time scales of 2–4 weeks. The complete results of this project will be presented later. In this paper, we report the discovery of discontinuities in the dynamic spectrum of the pulsar 0823+26. The discontinuities occur over time scales $\lesssim 2$ minutes and are accompanied by strong oscillatory modulations in the pulsar's light curve over time scales of ~ 15 minutes. To our knowledge such discontinuities have not been previously reported. We show that the discontinuities are a consequence of multiple imaging created by strong refraction, and we use the data to derive the characteristic angular separation between the images. Assuming the refraction is caused by a discrete object, we constrain the size of the object and its electron column density as a function of its distance along the line-of-sight. We briefly discuss the equally likely probability that the refraction is caused by the cumulative effect of many statistical fluctuations in the medium along the line-of-sight. Last, we note that 0823+26 is a good candidate for interstellar interferometry since it apparently undergoes extended periods of multiple imaging.

2. OBSERVATIONS

A set of pulsars was observed daily or every other day during three sessions, each spanning 2–4 weeks. The observations were conducted in 1988 June/July, 1988 October, and 1991 February using the 305 m Arecibo telescope.[4] Dynamic spectra were obtained at 430 and 1400 MHz in 1988 and at 130 MHz in 1991. Details of the data acquisition procedure can be found in Wolszczan & Cordes (1987). Nominally, the dynamic spectrum is dominated by diffractive intensity fluctuations caused by interstellar scattering. The fluctuations decorrelate over time and frequency with scales τ_d and $\Delta\nu_d$, respectively. The time and frequency resolution of our dynamic spectra were chosen to adequately sample the expected scintillation parameters of each pulsar; they ranged between 1 and 80 kHz per spectral channel and 2–30 s per time sample, with 512 spectral channels and ~ 200 time samples making up one dynamic spectrum. The following pulsars were monitored: 0611+22, 0823+26, 0834+06, 0919+06, 0950+08, 1133+16, 1237+25, 1737+13, 1842+14, 1915+13, 1919+21, 1929+10, 1933+16, and 2110+27.

The full results of this monitoring project will be discussed elsewhere. Here we report only the results for the pulsar 0823+26. Observations of 0823+26 were conducted at both 430 and 1400 MHz (not simultaneously) on 1988 June 8–12; at 430 MHz only on 1988 June 15, 17, 19, 24, 25, 27, 29, and 1988 July 3; and at 1400 MHz only on 1988 June 14, 16, 18, 20, 22, 26, and 1988 July 1, 4, and 6. We also observed 0823+26 at 130 MHz on 1991 February 12 and 15.

[1] Naval Research Laboratory, Code 7210, Washington, DC 20375-5351.
[2] NRC/NRL Cooperative Research Associate.
[3] Department of Astronomy, Cornell University, Ithaca, NY 14853-6801.

[4] Arecibo is part of the National Astronomy and Ionosphere Center which is operated by Cornell University under contract with the National Science Foundation.

3. RESULTS

At 1400 MHz, the pulsar routinely exhibited discontinuities in its scintillation pattern, accompanied by strong modulations in its light curve over the full 40 MHz bandwidth. Figure 1 shows one of the best examples of such an event. The changes in the dynamic spectrum occurred over time scales of ~ 2 minutes and the light curve oscillations had amplitudes as great as 100% and periods of ~ 10–30 minutes. These phenomena were observed to varying degrees in every 1400 MHz observation of the pulsar; additional examples are shown in Figure 2. At 430 MHz, no discontinuities and no broad-band oscillations were seen, although the dynamic spectra did show evidence for the narrow-band diagonal stripes commonly attributed to fringes caused by coherent interference between images (Cordes & Wolszczan 1986). At 130 MHz, the pulsar was too weak to produce a suitable dynamic spectrum. This is an unusual result in that previous observers report that 0823+26 is a strong emitter at frequencies near 130 MHz (e.g., Fig. 1 of Phillips & Wolszczan 1992).

4. DISCUSSION

We believe that the discontinuities in the dynamic spectrum of 0823+26 and the broad-band oscillations in its light curve are the result of strong refraction in the interstellar medium. In this section, we will assume that the refraction is caused by a discrete object and the analysis of the 0823+26 data will be developed in the following way: first, the basic refractive properties of an interstellar plasma lens will be derived; second, these properties will be utilized to deduce the angular splitting between images of the pulsar based on the observed oscillation time scale of the fringes in the pulsar's light curve; third, the magnitude of the angular separation will be used to constrain the physical characteristics of the lens; last, the angular splitting between the images and the physical characteristics of the lens will be used to deduce an explanation for the discontinuities in the dynamic spectrum.

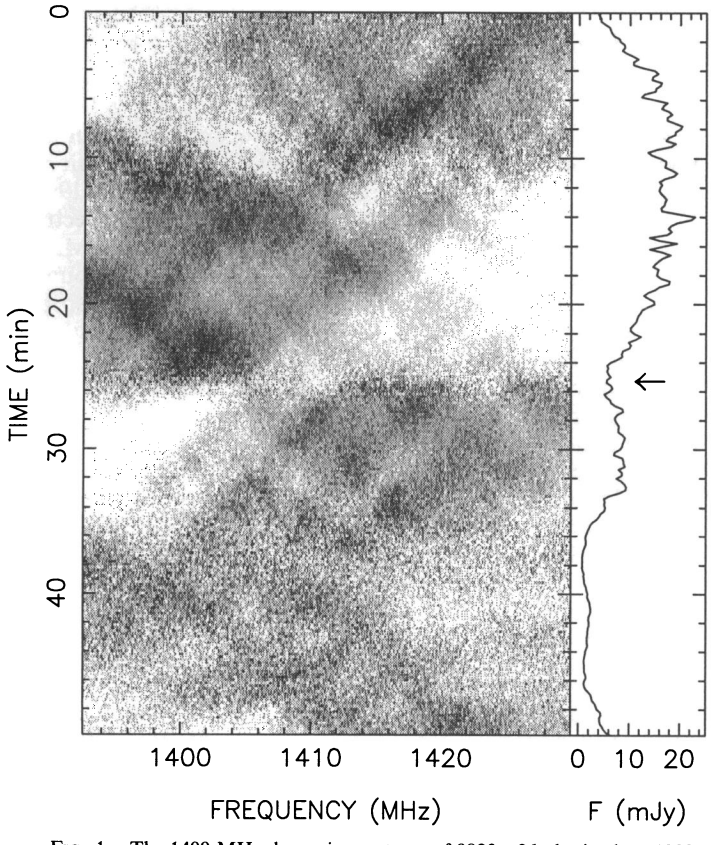

FIG. 1.—The 1400 MHz dynamic spectrum of 0823+26 obtained on 1988 July 4. The gray-scale levels indicate flux density (black means strong). The light curve, shown at right, was obtained by summing the dynamic spectrum over the entire bandwidth (the noiselike variations in the light curve on time scales of less than 1 minute are artifacts of the data reduction procedure). The discontinuity (marked with an arrow) occurs approximately 25 minutes after the start of the observation. At that time, the scintillation maximum near 1400 MHz undergoes an unusually sharp cutoff, and the scintillation minimum near 1420 MHz makes a sudden transition to a scintillation maximum.

4.1. *Physical Characteristics of the Lens System*

We consider a one-dimensional refracting screen with free-electron column density (aka dispersion measure) profile $DM(x)$ which lies between the Earth and the pulsar (Fig. 3). The coordinate x represents position along the refracting screen, and the coordinate x' denotes position along the observer's plane. The distance between the screen and the observer is z_1, while the distance from the screen to the pulsar is z_2. The Earth-pulsar distance is $D = z_1 + z_2$, where D is known to be 357 ± 80 pc from parallax measurements of Gwinn et al. (1986). The phase velocity in the plasma lens is greater than c, so the lens imparts a phase *advance* $\phi_l(x) = \lambda r_e DM(x)$ to the wave front from the pulsar, where λ is the observing wavelength and r_e is the classical electron radius. The phase disturbance results in refraction of the pulsar emission. In all interstellar applications the refraction is small, corresponding to angles $\lesssim 1$ mas at centimeter wavelengths, so that small-angle approximations can be used. A ray which is refracted from a point x on the lens screen which subsequently reaches the observer at a point x' undergoes a geometrical phase *delay* of magnitude $\phi_g(x, x')$. The total phase of a ray reaching the observer is $\Phi(x, x') = \phi_l(x) - \phi_g(x, x')$. The exact form of $\phi_l(x)$ is not important at the moment. The geometrical phase delay is

$$\phi_g(x, x') = \frac{2\pi D}{\lambda} + \frac{\pi}{\lambda}\left[\frac{x^2}{z_2} + \frac{(x - x')^2}{z_1}\right]. \quad (1)$$

If the rays are strongly refracted by the lens, ray crossing will occur and an observer at coordinate x' may see several images of the pulsar, each arriving from a different position x on the lens screen. There will generally be a phase difference between the images as each will have a different phase Φ.

For the following discussion, consider the phase difference between two images which have been created by the lens. Let the images be refracted from screen coordinates x_1 and x_2 to an observer at x'. The phase difference between the two images is

$$\Delta\Phi = \Phi_1 - \Phi_2 = \phi_l(x_1) - \phi_l(x_2) - \frac{\pi}{\lambda}\left[\frac{x_1^2}{z_2} + \frac{(x_1 - x')^2}{z_1} - \frac{x_2^2}{z_2} - \frac{(x_2 - x')^2}{z_1}\right]. \quad (2)$$

If the observing instrument does not resolve the images and the observing bandwidth is sufficiently small, the total observed intensity is formed from the coherent sum of the electric fields from the two images, which will be largest when $\Delta\Phi = 2n\pi$ (constructive interference) and smallest when $\Delta\Phi = (2n - 1)\pi$ (destructive interference), where n is an integer. The extrema of the observed intensity depend on the relative intensities of the

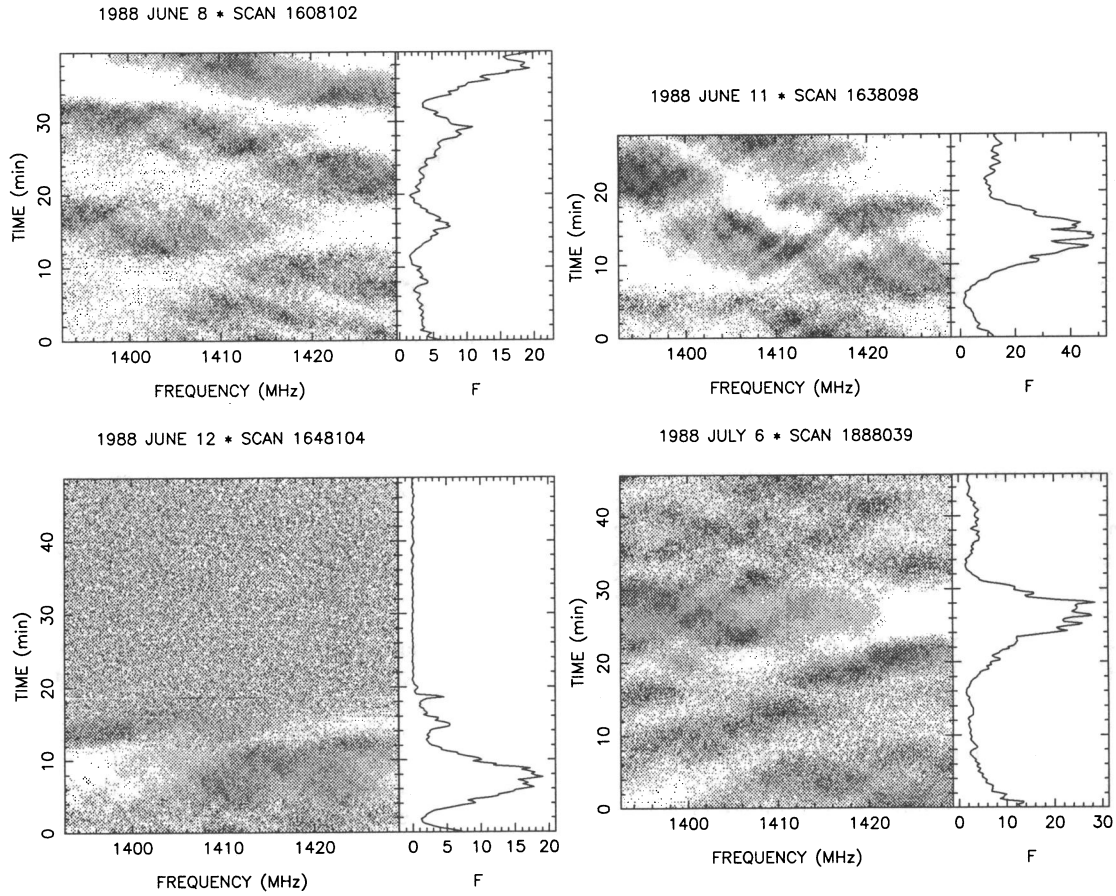

FIG. 2.—Additional examples of dynamic spectra obtained towards 0823+26 during 1988 June/July. The dynamic spectra show varying degrees of change in the scintillation pattern during the period of observation, although each displays large oscillations in the full 40 MHz light curve. The same scales along the frequency and time axes are used for each figure. (For display purposes, the data in this figure and in Fig. 1 have been renormalized so that the individual spectra which make up one dynamic spectrum have zero mean and unit standard deviation. This normalization makes the scintillation pattern more visible, but also causes periods of low flux density in the dynamic spectrum to appear noiselike with a full range of gray scales present. The broad-band light curves are computed before any renormalization of the data is performed, so they are not affected.)

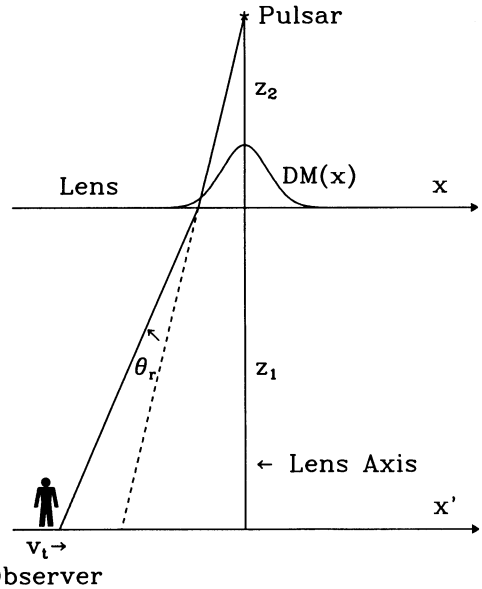

FIG. 3.—Geometry of the interstellar lens system. A discrete refractor represented by the profile $DM(x)$ is located a distance z_1 from the observer and a distance z_2 from the pulsar. A ray from the pulsar is refracted by the lens to reach the observer, who is located on the x' axis and is moving with transverse velocity $v_t = dx'/dt$ with respect to the lens. During multiple imaging events, rays from more than one point along the lens are refracted to the observer.

separate images, which may or may not be the same due to differential focusing or defocusing across the lens. If the images have the same intensity I_0, the maximum observed intensity will be $4I_0$ and the minimum will be 0.

The phase difference $\Delta\Phi$ between the two images will change as the observer moves along the x' axis across interferometric fringes created by beating between the two images. The projected fringe spacing $\delta x'_f$ (i.e., the distance between fringe maxima as projected onto the observer's plane) is

$$\delta x'_f \simeq 2\pi\left[\frac{d\Delta\Phi}{dx'}\right]^{-1} . \tag{3}$$

The apparent image locations x_1 and x_2 are functions of x', so the derivative in equation (3) must be written as a sum of partial derivatives:

$$\frac{d\Delta\Phi}{dx'} = \frac{\partial\Delta\Phi}{\partial x'} + \frac{\partial\Delta\Phi}{\partial x}\frac{dx}{dx'} . \tag{4}$$

From optics theory, the images appear to arrive from points where the phase Φ is stationary with respect to perturbations in x (cf. Born & Wolf 1980), so that $(\partial\Delta\Phi/\partial x) = 0$. Then

$$\frac{d\Delta\Phi}{dx'} = \frac{\partial\Delta\Phi}{\partial x'} = \frac{2\pi}{\lambda}\left(\frac{x_1 - x_2}{z_1}\right) \equiv \frac{2\pi}{\lambda}\,\delta\theta , \tag{5}$$

where $\delta\theta = (x_1 - x_2)/z_1$ is the apparent angular separation (in

radians) between the two images. The fringe spacing is then given by

$$\delta x'_f \simeq \frac{\lambda}{\delta\theta} . \tag{6}$$

If the observer passes through the fringe pattern with a transverse velocity $v_t = dx'/dt$, oscillations in the light curve will occur on a time scale $\delta t_f = \delta x'_f / v_t$. In this case, working backward from the observed oscillation time scale the angular separation between the images can be determined:

$$\delta\theta = \frac{\lambda}{\delta t_f v_t} . \tag{7}$$

We assume that the oscillations in the light curve of 0823+26 are due to coherent interference between images of the pulsar created by strong refraction. The light curve oscillations in Figures 1 and 2 do not strictly resemble the simple fringe pattern between two point sources because in reality more than two images are created by a refractor and each can have a different intensity. If n images are visible, $n(n-1)/2$ interference terms are created, so the total light curve may be quite complex, keeping in mind that the relative intensity of each image is changing as a function of x'.

In the broad-band light curve of 0823+26 (Fig. 1), we notice an increase in intensity starting at $t = 0$, followed by a maximum at $t \simeq 14$ minutes, a local minimum at $t = 25$ minutes, a local maximum at $t = 30$ minutes, and an extended period of diminished intensity after $t = 38$ minutes. (The noise-like variations in the light curve on time scales of less than 1 minute are artifacts of the data reduction procedure). The presence of local minima and maxima atop a light curve that exhibits an extended minimum leads us to believe that more than one oscillation time scale is present. In any event, each light curve obtained for 0823+26 shows a similar structure (see Fig. 2). The shorter time scale oscillations responsible for the local minima and maxima have oscillation periods of 10–30 minutes, with 15 minutes being typical.

Our transverse velocity with respect to the refractor is unknown. Cordes (1986) derived a scintillation velocity for 0823+26 of $v_{\rm iss} = 91 \pm 27$ km s^{-1}, where the scintillation velocity is the transverse velocity relative to the scattering material responsible for diffractive scintillation in the pulsar's dynamic spectrum. We will adopt the scintillation velocity as a reasonable estimate of v_t. Using equation (7) we find at $\lambda = 21$ cm that $\delta\theta \simeq 2.6 \times 10^{-9}$ rad $\simeq 0.5$ mas.

From the inference that multiple imaging is occurring and using the estimate of the angular separation between one pair of images, we can derive basic physical characteristics of the refractor. We assume that the refractor is a discrete object of transverse size a whose maximum free-electron column density is DM_0. The characteristic refraction angle imparted on an incident ray by such a structure is

$$\theta_r \simeq \frac{\lambda}{2\pi} \nabla\phi_l \simeq \frac{\lambda}{2\pi} \frac{\phi_{l,0}}{a} \simeq \frac{\lambda^2 r_e DM_0}{2\pi a} , \tag{8}$$

where $\phi_{l,0} = \lambda r_e DM_0$ is the characteristic phase perturbation imparted by the refractor, and the transverse gradient $\nabla\phi_l$ has been approximated by $\phi_{l,0}/a$.

The apparent angular size of the lens can be no less than the angular distance $\delta\theta$ between images that are created by the lens. This gives us a lower bound on the size of the refractor as a function of its distance z_1:

$$a \gtrsim z_1 \delta\theta . \tag{9}$$

Since ray crossing is occurring, the lens must refract rays to the extent that over a distance z_1 the displacement of the rays is greater than the transverse extent of the lens:

$$\theta_r z_1 = \frac{\lambda^2 r_e DM_0 z_1}{2\pi a} \gtrsim a . \tag{10}$$

When combined with equation (9), a lower limit on the characteristic column density through the lens is obtained as a function of the distance to the lens:

$$DM_0 \gtrsim \frac{2\pi \delta\theta^2 z_1}{\lambda^2 r_e} . \tag{11}$$

If we take the extent of the lens along the line-of-sight as ηa, where η is an "elongation factor," the electron density of the refractor is constrained to be

$$n_e \gtrsim \frac{DM_0}{(\eta a)} = \frac{2\pi\delta\theta}{\eta\lambda^2 r_e} . \tag{12}$$

If we assume that the lensing is caused by a single discrete object, we can use these formulae to constrain the physical characteristics of the lens responsible for the strong refraction of 0823+26. Given that $\delta\theta \simeq 0.5$ mas, and defining $z_1 \equiv fD$, where $D = 357$ pc is the distance to the pulsar and f is the fractional distance to the lens along the line-of-sight to the pulsar, we get

$$a_{\rm min} = 0.19 f \ {\rm AU} ; \tag{13}$$

$$DM_{0,\rm min} = 1.2 \times 10^{-4} f \ {\rm cm}^{-3} \ {\rm pc} . \tag{14}$$

The minimum electron density as a function of η is

$$n_{e,\rm min} = 123/\eta \ {\rm cm}^{-3} . \tag{15}$$

4.2. *The Dynamic Spectrum Discontinuities*

The above analysis of the lens system responsible for strong refraction of the pulsar 0823+26 finally leads us to a qualitative explanation for the origin of the discontinuities in the pulsar's dynamic spectrum. We have established that the pulsar is undergoing multiple imaging as evidenced from the interference fringes in its light curve, and from those fringes we estimate that the angular splitting between the images is roughly 0.5 mas.

Each of the two or more images of the pulsar travels a different optical path to reach the observer. Furthermore, each of these images will possess different diffractive scintillation patterns, since the small-scale electron density fluctuations encountered over each optical path are different. If the statistics of the fluctuations are the same along each path and the path-length difference is a small fraction of the total path length, then the observable interstellar scattering parameters such as Δv_d and τ_d (the scintillation bandwidth and time scale) for each image will be the same. That is, if each image could be observed alone (using an interferometer, for example), then the observed decorrelation time and frequency scales for the images will be comparable to one another. What will be different for each image, however, is the location in the time/frequency domain of the scintillation maxima and minima. This is true because the diffraction patterns of each image will be offset from one another since the images themselves are

spatially offset, as seen by the observer. The exact offset between the diffraction patterns is difficult to determine since it depends on the true geometry of observer, lens, and pulsar, but to a zeroth order approximation, the offset is comparable to the apparent spatial offset $z_1 \delta\theta$ between the images. The refractive splitting angle $\delta\theta$ is greater than diffractive angular scales, since otherwise multiple imaging would not be evident (the refractive splitting angle would be less than the diffractively broadened image size). Consequently, the spatial offset $z_1 \delta\theta$ between diffraction patterns will be greater than the decorrelation length scale for the diffractive scintillations, which is set by diffractive angular scales.

We believe this is the origin of the discontinuities observed in the dynamic spectrum of 0823+26. The pulsar is undergoing multiple imaging, with each of the images forming a separate scintillation pattern. Since we are observing with a single-dish instrument, the separate images are not resolved, so the observed scintillation pattern is formed from the sum of the scintillation patterns of each of the images. Over bandwidths less than or comparable to the characteristic scintillation bandwidth for the images, the dynamic spectrum is formed from the *coherent* sum of the individual scintillation patterns. This is the case in our observations of 0823+26 since the pulsar's scintillation bandwidth at 1400 MHz is not much smaller than our observing bandwidth of 40 MHz, judging from the dynamic spectrum.

It follows, therefore, that our observed dynamic spectrum is alternately dominated by the scintillation pattern of various images, as these images interfere constructively and destructively with one another. Consider the case of three images of the pulsar: when two images with equal intensities interfere destructively with each other, their combined emission temporarily drops out, leaving only the emission from the third image, whose scintillation pattern alone will then dominate the observed dynamic spectrum. In reality the situation is more complicated since each image may have a different intensity, but the net effect is the same: the dynamic spectrum will periodically undergo sudden changes as different images dominate the received intensity.

How fast the dynamic spectrum will change is difficult to determine. We can derive a lower limit to the transition time scale, based on the maximum resolution of the lens system. Consider that a lens of size a has a diffractive angular resolution of no better than $\sim\lambda/a$. Over a distance z_1 this corresponds to a spatial resolution no better than $\sim(\lambda/a)z_1$. We therefore expect that there cannot be any changes imparted by the plasma lens in the light curve or dynamic spectrum that occur over time scales shorter than $\sim(\lambda/a)z_1/v_t$. Using $v_t = 91$ km s^{-1} and assuming that the lens is located halfway to the pulsar ($z_1 = 180$ pc) with a size of $a = 0.1$ AU (which from eq. [13] is the minimum lens size for this distance), we find an approximate "diffraction-limited" time scale of 14 minutes for a lens of this size at this distance.

The observed transition time in the 0823+26 dynamic spectrum is roughly 2 minutes. This is shorter than the nominal case worked out in the preceding paragraph, but can easily be explained if we assume the lens is larger than the minimum size of 0.1 AU. For example, a lens of size $\sim$0.7 AU located halfway to the pulsar has a diffraction-limited time scale for fluctuation of approximately 2 minutes. Alternatively, the 2 minute time scale is consistent with a lens smaller than 0.7 AU located closer than halfway to the pulsar, or a lens larger than 0.7 AU located farther than half the pulsar distance away. In any event, the discontinuities in the dynamic spectrum of 0823+26, as well as the oscillatory modulations in the pulsar's broadband light curve, are qualitatively consistent with the effects of strong interstellar refraction leading to multiple imaging.

4.3. *Further Considerations*

We note that the derived constraint on the electron density of the refractor is comparable to that derived for the localized plasma structures that may be responsible for the extreme scattering events of extragalactic sources (Fiedler et al. 1987; Romani, Blandford, & Cordes 1987). However, the minimum column density we derive is nearly three orders of magnitude less than that derived by Romani et al. for the extreme scatterers. This result reflects the fact that stronger refractors are required to create multiple images of extragalactic sources than for pulsars—the splitting angle must be greater than the intrinsic angular size of the source, which is $\sim$1 mas for extragalactic objects, but $\sim$1000 times smaller for pulsars. The excess dispersion measure added by the refractor described in this paper is as small as $\sim 10^{-4}$ cm^{-3} pc, which is undetectable in even the most sensitive observations of dispersion measure variations towards 0823+26 (Phillips & Wolszczan 1991).

Clegg & Fiedler (1992) have been performing detailed numerical simulations of refractive and diffractive imaging effects by one-dimensional Gaussian plasma lenses [lenses with Gaussian profiles in $DM(x)$]. The similarity in the oscillatory light curves resulting from these simulations and those observed for 0823+26 led to the principle approach adopted in this paper. One salient result from the simulations is the realization that the volume of space over which multiple imaging is visible can be very large. The often-used approximation that the size of the lens must be comparable to the duration of a lensing event times a characteristic transverse velocity of the pulsar/lens/observer system is incorrect. For example, a lens with maximum column density $DM_0 = 0.01$ cm^{-3} pc, size $a = 0.5$ AU, at a distance $z_1 = 250$ pc, results in multiple images that are visible over approximately 10 AU at $\lambda = 21$ cm, and 100 AU at $\lambda = 70$ cm. An observer moving with a transverse velocity of 100 km s^{-1} with respect to the lens-pulsar reference frame would see multiple images over a time span of 0.5 and 5 yr, respectively, so the 1 month period in which we routinely detected multiple imaging effects in the 0823+26 data is not surprising with respect to discrete lens models. The time scales will differ depending on whether the transverse velocity of the observer-pulsar, observer-lens, or lens-pulsar reference frames dominate, but the simulations show that substantial periods of strong refraction can be created in most cases. For an observer moving with respect to a fixed lens-pulsar reference frame, the extent of the multiple imaging region scales roughly with $\lambda^2 DM_0 z_1/a^2$, so sharp lenses (small a) with large DM_0, perhaps created by a shock front (Clegg, Chernoff, & Cordes 1988) or by stellar winds, will create multiple images which are visible over very large regions of space.

The behavior of 0823+26 at 430 and 130 MHz is consistent with the strong refraction picture presented here. At 430 MHz, the data show evidence for fringing due to coherent interference, although the bandwidth for the fringing is much narrower than the scintillation bandwidth so no discontinuities in the scintillation pattern are evident. The low flux density of 0823+26 at 130 MHz in 1991 February may be caused by an extended period of refractive defocusing by the same medium responsible for the fringing at 430 and 1400 MHz. Refractive

effects are stronger at the longer wavelengths, so time scales for fringing are expected to be longer at 130 MHz, although additional data and simulations are required to work out the exact form of the wavelength scaling of these multiple imaging phenomena.

Other nearby pulsars exhibit strong refraction effects, such as fringing in their dynamic spectra, most of the time (although to our knowledge discontinuities in the dynamic spectra of these pulsars have not been observed). Two examples are 0834+06 and 1133+16, at approximate distances of 430 and 160 pc, respectively. More distant pulsars tend not to exhibit frequent occurrences of strong refraction. It is plausible, then, that the origin for the refraction lies relatively nearby. Phillips & Clegg (1992) recently measured the degree of scattering inside of the local superbubble and found that the turbulence level inside the bubble is very low. They concluded that any turbulence created by the bubble may be localized to the interface between the bubble and the ambient warm ISM. It is possible, then, that such a turbulent interface is the origin of the strong refraction of nearby pulsars.

We note that strong refraction may arise not from a discrete object, but from the cumulative effect of large fluctuations in the ionized interstellar medium along the line-of-sight. Fiedler et al. (1993) proposed such an origin for the extreme scattering events, in contrast to the discrete refractor model offered by Romani et al. (1987). Without additional information we are unable to suggest any evidence favoring one model over the other, partly because the two models are not entirely independent: the discrete refractor model is the limit of the strong fluctuation model when only one large fluctuation dominates the refraction.

Last, it is evident that the spectrum of electron density fluctuations toward 0823+26 cannot be Kolmogorov, as is suggested along many other lines of sight by scintillation and scattering measurements of a number of sources. The reason is that a Kolmogorov spectrum of irregularities does not give rise to multiple imaging, while our observations of 0823+26 clearly suggest multiple imaging is occurring.

5. CONCLUSIONS

The pulsar 0823+26 has been undergoing a variety of effects consistent with strong refraction in the interstellar medium. One of the most curious effects is that the 1400 MHz dynamic spectrum frequently exhibits discontinuities where the scintillation pattern changes form over time scales of $\sim$2 minutes. The changes in the dynamic spectrum are accompanied by strong oscillations in the pulsar's broad-band (40 MHz) light curve. We believe both effects are due to beating between images of the pulsar created by the interstellar lens, and we are able to estimate that the angular splitting between the images is $\sim$0.5 mas. The discontinuities occur as different images, or combinations of images, beat together and alternately dominate the received intensity. The images each travel a different ray path and their diffraction patterns are offset from one another by more than a diffractive length scale, so their scintillation patterns will be distinct from one another. As the various images alternately dominate the received intensity, therefore, we expect discontinuous changes in the observed scintillation pattern.

If the refractor is a discrete object, its extent transverse to the line-of-sight is $\gtrsim 0.19f$ AU, and its electron column density is $\gtrsim 1.2 \times 10^{-4} f\,\mathrm{cm}^{-3}$ pc, where f is the fractional distance of the object along the line-of-sight. The electron density within the refractor is $\gtrsim 123/\eta\ \mathrm{cm}^{-3}$, where η is the elongation of the object along the line-of-sight relative to its transverse dimension. A single, discrete refractor may not be the source of the refraction. A statistical model in which the refraction is the cumulative effect of a number of electron density fluctuations along the line-of-sight may instead be appropriate. In either case, the spectrum of electron density fluctuations along the line-of-sight to 0823+26 is not Kolmogorov, since such a spectrum does not give rise to multiple imaging.

Because 0823+26 apparently undergoes extended periods of fringing due to multiple imaging, it is a promising candidate for the interstellar interferometry technique demonstrated by Wolszczan & Cordes (1987). The data described here do not have sufficient time resolution across the pulse to apply this technique, but we are currently in the process of obtaining additional data.

The authors thank Tony Phillips for comments on the manuscript. A. W. C. is supported by a National Research Council/Naval Research Laboratory Cooperative Research Associateship.

REFERENCES

Born, M., & Wolf, E. 1980, Principles of Optics (Oxford: Pergamon), 386
Clegg, A. W., Chernoff, D. F., & Cordes, J. M. 1988, in Radio Wave Scattering in the Interstellar Medium (AIP Conf. Proc 174), ed. J. Cordes, B. Rickett, & D. Backer (New York: AIP), 174
Clegg, A. W., & Fiedler, R. L. 1992, work in progress
Cordes, J. M. 1986, ApJ, 311, 183
Cordes, J. M., & Wolszczan, A. 1986, ApJ, 307, L27
Fiedler, R. L., Dennison, B., Johnston, K. J., & Hewish, A. 1987, Nature, 326, 675
Fiedler, R. L., Dennison, B., Johnston, K. J., Waltman, E. B., & Simon, R. S. 1993, ApJ, submitted
Gwinn, C. R., Taylor, J. H., Weisberg, J. M., & Rawlings, L. A. 1986, AJ, 91, 338
Phillips, J. A., & Clegg, A. W. 1992, Nature, 360, 137
Phillips, J. A., & Wolszczan, A. 1991, ApJ, 382, L27
———. 1992, ApJ, 385, 273
Rickett, B. J. 1990, ARA&A, 28, 561
Romani, R. W., Blandford, R. D., & Cordes, J. M. 1987, Nature, 328, 324
Wolszczan, A., & Cordes, J. M. 1987, ApJ, 320, L35